POLISH POLAR RESEARCH
vol. 35, no. 2, pp. 151–176, 2014 doi: 10.2478/popore-2014-0021

Marine environment around Iceland: hydrography, sediments and first predictive models of Icelandic deep-sea sediment characteristics

Alexandra OSTMANN[1] *, Sarah SCHNURR[2] and Pedro MARTÍNEZ ARBIZU[1]

[1] *Senckenberg am Meer, Dept. Deutsches Zentrum für Marine Biodiversitätsforschung (DZMB), Südstrand 44, 26382 Wilhelmshaven, Germany*

[2] *Senckenberg am Meer, Dept. Deutsches Zentrum für Marine Biodiversitätsforschung (DZMB), c/o Biozentrum Grindel, Martin-Luther-King Platz 3, 20146 Hamburg, Germany*

* *corresponding author <aostmann@senckenberg.de>*

Abstract: Sediment samples and hydrographic conditions were studied at 28 stations around Iceland. At these sites, Conductivity-Temperature-Depth (CTD) casts were conducted to collect hydrographic data and multicorer casts were conducted to collect data on sediment characteristics including grain size distribution, carbon and nitrogen concentration, and chloroplastic pigment concentration. A total of 14 environmental predictors were used to model sediment characteristics around Iceland on regional scale. Two approaches were used: Multivariate Adaptation Regression Splines (MARS) and randomForest regression models. RandomForest outperformed MARS in predicting grain size distribution. MARS models had a greater tendency to over- and underpredict sediment values in areas outside the environmental envelope defined by the training dataset. We provide first GIS layers on sediment characteristics around Iceland, that can be used as predictors in future models. Although models performed well, more samples, especially from the shelf areas, will be needed to improve the models in future.

Key words: Icelandic waters, MARS and randomForest models, sediments, IceAGE project.

Introduction

The description of the marine environment is pivotal for understanding species distributions, and benthic standing stocks and biodiversity patterns. In the absence of light, the deep-sea benthos depends on the input of organic matter produced at the ocean surface, at least in regions where no chemoautotrophic systems, such as hot and cold vents, wood falls and whale falls, are present (*e.g.* Danovaro *et al.* 2001). Other factors structuring benthic biodiversity are water depth, temperature and salinity, dissolved oxygen, topography, distance from the coast and bottom currents (Thistle *et al.* 1985; Rex *et al.* 2005, 2006; Smith *et al.* 2008).

Environmental layers are modeled continuous datasets on environmental conditions over geographic space. This information is needed to calculate models on species distributions and model ecosystem functions (biomass, diversity etc) at regional scale. For marine habitats this kind of environmental information is often scarce or only available at global-scale resolution, lacking detail for regional studies.

The marine fauna around Iceland has been studied intensively thanks to the BIOICE project (Benthic Invertebrates of Icelandic waters, 1991–2004), which focused on studying the benthic invertebrates and their ecology around Iceland (Svavarsson *et al*. 1993; Weisshappel and Svavarsson 1998; Brix and Svavarsson 2010; Schnurr *et al.* 2014).

The IceAGE (Icelandic marine Animals: Genetics and Ecology, since 2011) project, builds on the BIOICE project by adding and combining the modern aspects of biodiversity research such as phylogeography (population genetics and DNA barcoding) and species distribution models (Meißner *et al*. 2014) with classic taxonomy.

Considering the seas around Iceland continuous environmental layers were only available for a small number of predictors like depth, oxygen, currents, temperature and salinity. But GIS layers on sediment characteristics were lacking so far. The aim of this study is to produce first predictive models on sediment characteristics around Iceland by analyzing a set of sediment samples taken by ourselves along depth gradients on Icelandic waters. The present study contributes to the IceAGE project by 1) summarizing the environmental data (hydrography, sediment grain size, sediment organic matter) collected during the summers of 2011 and 2013 around Iceland, and 2) predicting the seabed sediments on a larger spatial scale using regression (MARS) and tree-based (randomForest regression) models. The results will be for species diversity and ecological modeling along depth gradients and geographical barriers. Supplementary data in the form of grid-files, figures without 300 m, *m* exclusion, data table are provided in the Pangaea information system (http://dx.doi.org/10.1594/PANGAEA.831943).

Materials and methods

Study site. — The study area covers the northernmost North Atlantic and the south-western part of the Greenland, Iceland and Norwegian Seas (GIN Seas, Fig. 1). The Greenland-Scotland Ridge (GSR) extends from West to East, featuring a mean depth of less than 500m and three deep sills (Fig. 1). According to several studies on physical oceanography around Iceland, the main deep water masses in the study area are Arctic Water (AW), Polar Water (PW, notable at the surface), Labrador Sea Water (LSW), Modified North Atlantic Water (MNAW), Norwegian Sea Arctic Intermediate Water (NSAIW) and Norwegian Sea Deep Water (NSDW) (Stefánsson 1962; Hansen and Østerhus 2000; Malmberg and Valdimarsson 2003).

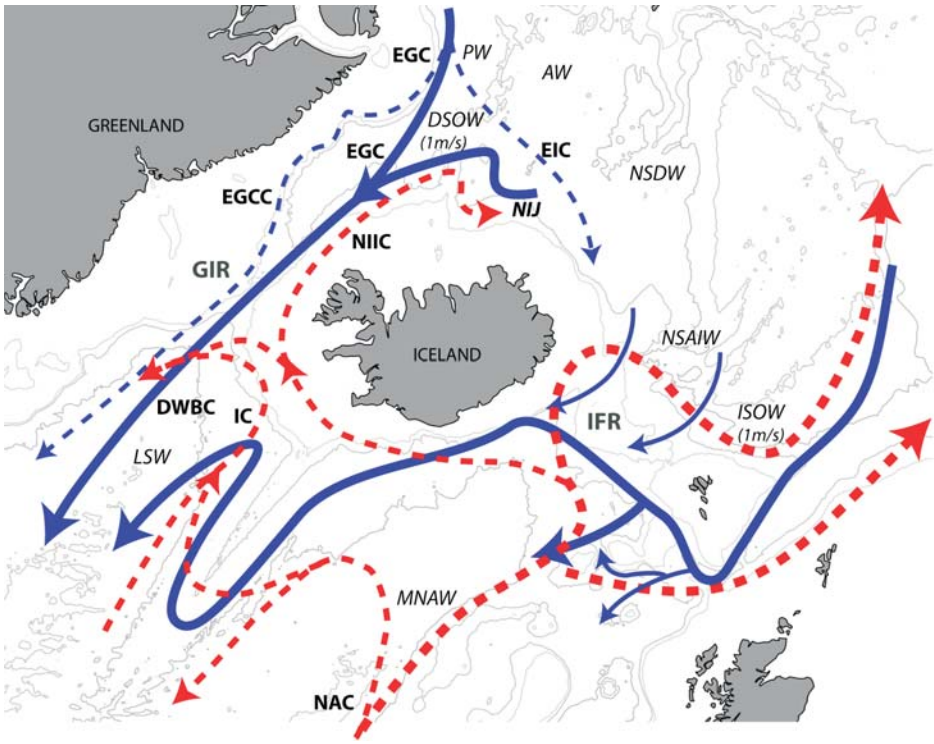

Fig. 1. Overview of the currents and water masses present in the study area (see Swift 1980; Swift and Aagaard 1984; Swift *et al.* 1984; Hansen and Østerhus 2000; Pickart *et al*. 2005; Logemann *et al*. 2013; Våge *et al*. 2013). Blue continuous arrows indicate cold deep water currents and waters. Blue dashed arrows refer to cold surface currents. Red dashed arrows display warm surface currents. Letters in italics refer to water masses, letters in bold indicate currents and the ridge parts. AW, Arctic Water; DSOW, Denmark Strait Overflow Water; DWBC, Deep Water Boundary Current; EGC, East Greenland Current; EGCC, separated East Greenland Current; EIC, East Icelandic Current; GIR, Greenland-Iceland Ridge; IC, Irminger Current; IFR, Iceland-Faroe Ridge; ISOW, Iceland Scotland Overflow Water; MNAW, Modified North Atlantic Water; NAC, North Atlantic Current; NIIC, North Icelandic Irminger Current; NIJ, North Icelandic Jet; NSAIW, Norwegian Sea Arctic Intermediate Water; NSDW, Norwegian Sea Deep Water; LSW, Labrador Sea Water; PW, Polar Water.

West of Iceland, cold and less saline water is transported across the Greenland-Iceland Ridge (GIR) into the Atlantic as Denmark Strait Overflow Water (DSOW, Fig. 1), which flows along the Greenlandic coast as the Deep Water Boundary Current (DWBC). The surface East Greenland Current (EGC) transports PW across the ridge (Fig. 1). In the east of Iceland cold water is transported across the Iceland-Faroe Ridge (IFR) as Iceland Scotland Overflow Water (ISOW, Fig. 1), which flows along the Reykjanes Ridge into the Irminger Basin (Swift 1980; Swift and Aagaard 1981; Swift *et al.* 1984; Hansen and Østerhus 2000; Pickart *et al*. 2005; Logemann *et al.* 2013; Våge *et al.* 2011, 2013).

Due to geostrophic forces, there is a warm water inflow from the Atlantic into the Arctic Ocean. Two surface currents, the North Icelandic Irminger Current

(NIIC) and the North Atlantic Current (NAC), transport Modified North Atlantic Water (MNAW) into the Arctic Ocean (Fig. 1).

Sample collection, processing and data analyses. — A total of 28 samples were included in the present study, collected during two IceAGE expeditions. During IceAGE1, samples were taken on board of the German R/V *Meteor* (M85/3) in the Iceland Basin, Irminger Basin, Denmark Strait and Norwegian Sea from August to September 2011 (Fig. 2, 24 samples). The IceAGE2 cruise on board the German R/V *Poseidon* (POS456; August 2013) was located around the IFR (Fig. 2, 4 samples). A SeaBird CTD (Conductivity Temperature Depth) and a MUC (multicorer) were used to take hydrographic and sediment data, respectively. Samples were taken in depths between 300–3000m from the shelf to the abyss.

Hydrography and sediments. — Hydrographic parameters (temperature, salinity and oxygen) of each sampling area were measured during the IceAGE expeditions using a CTD. The CTD was handled during both cruises in the same way. The CTD data were processed using SBE Data Processing (Seasoft V2 software suite, 2013; http://www.seabird.com/) and evaluated using Matlab 2012a. Near-bottom measurements (10–20 m above the seafloor) of the stations were allocated to the water masses according to Stefánsson (1962), Hansen and Østerhus (2000) and Malmberg and Valdimarsson (2003).

Sediment samples were taken with the MUC. One core of each deployment was used for the analyses. The core was cut into 1 cm slices from top to 5 cm depth. Samples were analyzed for total organic carbon(TOC), nitrogen (N), chlorophyll *a* and pigment derivates, as well as sediment grain size distribution. However, only the first centimeter was used for the present study.

For the TOC, nitrogen and pigment analyses, sediments were lyophilized and homogenized at 300 rpm for 5 minutes and 160 rpm for 8 minutes. TOC and N were analyzed using 30 mg of the ground sediments (Nieuwenhuize *et al.* 1994). Removal of $CaCO_3$ was done by adding 1N HCl (Cutter and Radford-Knoery 1991) until bubble formation stopped. Then samples were dried over night at 40°C and analyzed with a C/N combuster (FLASH EA1112/Thermo, ICBM, Terramare, Wilhelmshaven).

An amount of 7 ml acetone was added to 5 g of the sediment to dissolve the pigments (*e.g.* Brown *et al.* 1981). After mixing and ultra-sounding, the sample was cooled and kept dark for at least 3 hours, followed by centrifugation. Pigments in the sediments were measured by injecting 250 µl of the supernatant into the HPLC (High Performance Liquid Chromatography) system (LaChrom L-7100, Diode Array Detector L-7450, flow 0.800, 65 minutes, EZ ChromElite software, ICMB Terramare, Wilhelmshaven).

For sediment grain size distribution samples were mixed homogenously. Sediments in grain size classes from 0.4 to 2000 µm were determined with a laser diffraction particle size analyzer (Beckman Coulter LS 13320) in the laboratory of MARUM (Center for Marine Environmental Sciences) in Bremen. From the over-

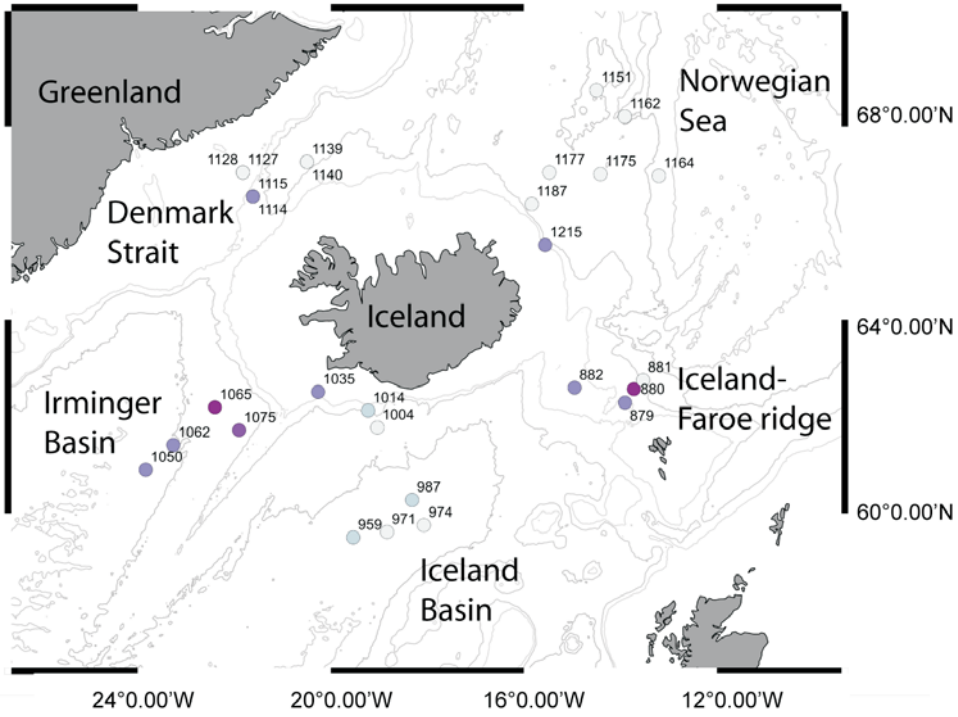

Fig. 2. Overview on the study site including the different stations and regions. The color code indicate the sediment grain size classification after Shepard (1954). See Fig. 4 for color description. Note the coarser grain sizes in the shelf regions and the Irminger Basin.

all distributions, grain size classes selected for this study are sand (2000–63 μm), silt (63–4 μm) and clay (<4 μm), according to the Udden-Wentworth scale (Wentworth 1922) and the classification was used according to Shepard (1954).

To compare the variation of the environmental data among the sampling sites, multivariate analyses were performed. The dataset was normalized in order to unify the range of the variables. An Analysis of Similarity (ANOSIM) was performed using the R© software packages *MASS* and *vegan* (Venables and Ripley 2002; Oksanen *et al.* 2013), based on a Bray-Curtis dissimilarity analysis. The dataset was categorized into "North-South" and five areas (Norwegian Sea, Iceland-Faroe Ridge, Iceland Basin, Irminger Basin and Denmark Strait). Moreover, the dataset was divided into depth gradients (upper slope [0–750 m], mid slope [751–1500 m], low slope [1501–2000 m], continental rise [2001–3000 m]).

Predictive models. — The second part of this study aimed at predicting the deep-sea sediment characteristics with a set of environmental layers of regional scale. A total of 14 layers were used as predictors (see Meißner *et al.* 2014 for a detailed description of some layers), including bottom depth (GEBCO_08 layer, 30 arc seconds resolution from www.gebco.net), bottom salinity and temperature including temperature maximum and inter-annual temperature range variation (Norwegian Iceland

Seas Experiment NISE; 1998–2008; Nilsen *et al.* 2008), bottom oxygen (Seiter *et al.* 2005), POC flux to the bottom and the seasonal variation index (SVI) of POC flux (Lutz *et al.* 2007), sediment thickness (NOAA, Divins 2003) and bottom currents.

Values of these layers at IceAGE multicore stations were extracted using the point sampling tool of QGIS (version 2.0.1; http://qgis.osgeo.org). A set of 22139 regular points were generated with QGIS for prediction. MARS models (Friedman 1991) were calculated using the "earth" package in R (Milborrow 2014). Interaction between predictors was allowed to up to 6 degrees.

In addition to the MARS models, randomForest regression models were calculated using the same predictors. RandomForest (Breiman 2001) is a machine learning technique using bagging to produce an ensemble of decision trees produced by recursive partitioning with a random selection of variables and observations each time. The R package randomForest (Liaw and Wiener 2002) with 3000 random trees and 4 random variables ("mtry" option) was used for generating the models. These were subsequently used to calculate the values on the prediction dataset described above.

Maps were generated with the Generic Mapping Tools (GMT 5.1.0, SOEST; http://gmt.soest.hawaii.edu/doc/5.1.0/). Interpolation was achieved with the "surface" function (continuous curvature surface gridding algorithm) using tension factor 0.5 and gridding space 0.005 degrees. The shallow, coastal areas above 300 m depth were excluded (clipped *a posteriori*, as grey-shaded areas within the figures), because no data were collected from the shelf areas during the IceAGE cruises. Black areas in the figures show where the models display values below the indicated scale and white areas display values above the indicated scale.

Abbreviations. — ADCP, Acoustic Doppler Current Profiler; ANOSIM, Analysis of Similarity; AW, Arctic Water; BIOICE, Benthic Invertebrates of Icelandic waters; CTD, Conductivity Temperature Depth; DSOW, Denmark Strait Overflow Water; DWBC, Deep Water Boundary Current; EGC, East Greenland Current; EGCC, separated East Greenland Current; EIC, East Icelandic Current; GIR, Greenland-Iceland Ridge; GSR, Greenland-Scotland Ridge; HPLC, High Performance Liquid Chromatography; IC, Irminger Current; IceAGE, Icelandic marine Animals: Genetics and Ecology; IFR, Iceland-Faroe Ridge; ISOW, Iceland Scotland Overflow Water; MARS, Multiple Adaptation Regression Splines; MNAW, Modified North Atlantic Water; MUC, multicorer; NAC, North Atlantic Current; NIIC, North Icelandic Irminger Current; NIJ, North Icelandic Jet; NSAIW, Norwegian Sea Arctic Intermediate Water; NSDW, Norwegian Sea Deep Water; LSW, Labrador Sea Water; PW, Polar Water.

Results

The results of this study are divided into two parts. First, the environmental conditions during the sample collection are presented. The second part of the results fo-

cuses on the MARS and randomForest predictive modeling approaches performed on the sediment grain sizes, organic material, chlorophyll *a* and pigment derivates.

Hydrographic and sediment conditions during the IceAGE expeditions. — The multivariate analysis performed on the sediment and hydrographic data show significant differences between the North and the South ($p = 0.001$, $R = 0.81544$, Fig. 3A), the five regions ($p = 0.001$ and $R = 0.8253$, Fig. 3B) and the depth gradients ($p = 0.001$, $R = 0.4981$, Fig. 3C). In the northeastern Norwegian Sea, where the bottom temperature and salinity (T: <-0.5°C, S: 34.91) are identified as NSDW (Table 1), the sediments are classified as clayey silt (~60–70% silt, Fig. 4, Table 2). The TOC (excluding station #1215) content in that region increases from 1.01% at the shelf to 5.26% in the deep sea, whereas the nitrogen and chlorophyll *a* content in the

Table 1

Hydrographic data at the seafloor sampling sites. Water masses are allocated according to Stefánsson (1962), Hansen and Østerhus (2000) and Malmberg and Valdimarsson (2003).

CTD number	MUC number	Date	Longitude	Latitude	Depth [m]	Temp [°C]	Salinity	Oxygen [µmol/kg]	Water mass
958	959	28 Aug 2011	-21.5	60.05	2749	2.75	34.99	254.42	MNAW
970	971	29 Aug 2011	-19.89	60.18	2670	2.71	34.99	256.26	MNAW
973	974	30 Aug 2011	-18.14	60.34	2563	2.66	34.99	258.64	MNAW
986	987	31 Aug 2011	-18.7	60.93	2493	2.30	34.99	261.34	MNAW
1000	1004	02 Sep 2011	-20.35	62.56	1392	3.88	35.02	254.62	MNAW
1013	1014	03 Sep 2011	-20.79	62.93	911	5.29	35.08	242.89	MNAW
1027	1035	04 Sep 2011	-23.17	63.33	307	8.02	35.23	241.66	MNAW
1049	1050	05 Sep 2011	-31.37	61.62	2528	3.16	34.94	254.12	LSW
1062	1062	08 Sep 2011	-30.06	62.17	1928	3.27	34.94	253.47	LSW
1064	1065	08 Sep 2011	-28.08	63	1619	4.28	34.99	245.57	LSW/MNAW
1074	1075	09 Sep 2011	-26.93	62.5	1175	4.37	35.00	244.52	LSW/MNAW
1112	1114	13 Sep 2011	-26.27	67.21	684	0.07	34.91	293.00	A/PW
1112	1115	13 Sep 2011	-26.27	67.21	684	0.07	34.91	293.00	A/PW
1127	1127	14 Sep 2011	-26.75	67.65	320	0.70	34.63	290.55	A/PW
1127	1128	14 Sep 2011	-26.75	67.65	320	0.70	34.63	290.55	A/PW
1138	1139	15 Sep 2011	-23.7	67.84	1238	-0.67	34.91	278.94	NSDW
1138	1140	15 Sep 2011	-23.7	67.84	1240	-0.67	34.91	278.94	NSDW
1150	1151	17 Sep 2011	-9.93	69.09	2270	-0.75	34.91	266.79	NSDW
1161	1162	18 Sep 2011	-8.58	68.64	1962	-0.80	34.91	272.77	NSDW
1163	1164	18 Sep 2011	-6.96	67.59	2403	-0.82	34.91	271.02	NSDW
1174	1175	20 Sep 2011	-9.74	67.62	1711	-0.76	34.91	267.93	NSDW
1176	1177	20 Sep 2011	-12.17	67.65	1820	-0.77	34.91	265.78	NSDW
1186	1187	21 Sep 2011	-13.01	67.07	1581	-0.74	34.91	269.12	NSDW
1214	1215	22 Sep 2011	-12.37	66.3	733	-0.40	34.90	283.03	NSAIW
879	879	31 Jul 2013	-8.57	63.1	510	1.33	34.95	305.41	MNAW/NSAIW
880	880	31 Jul 2013	-8.15	63.39	683	-0.43	34.91	306.67	NSAIW
881	881	01 Aug 2013	-7.71	63.58	1043	-0.58	34.91	304.44	NSAIW
882	882	02 Aug 2013	-10.97	63.42	440	0.27	34.91	311.95	NSAIW

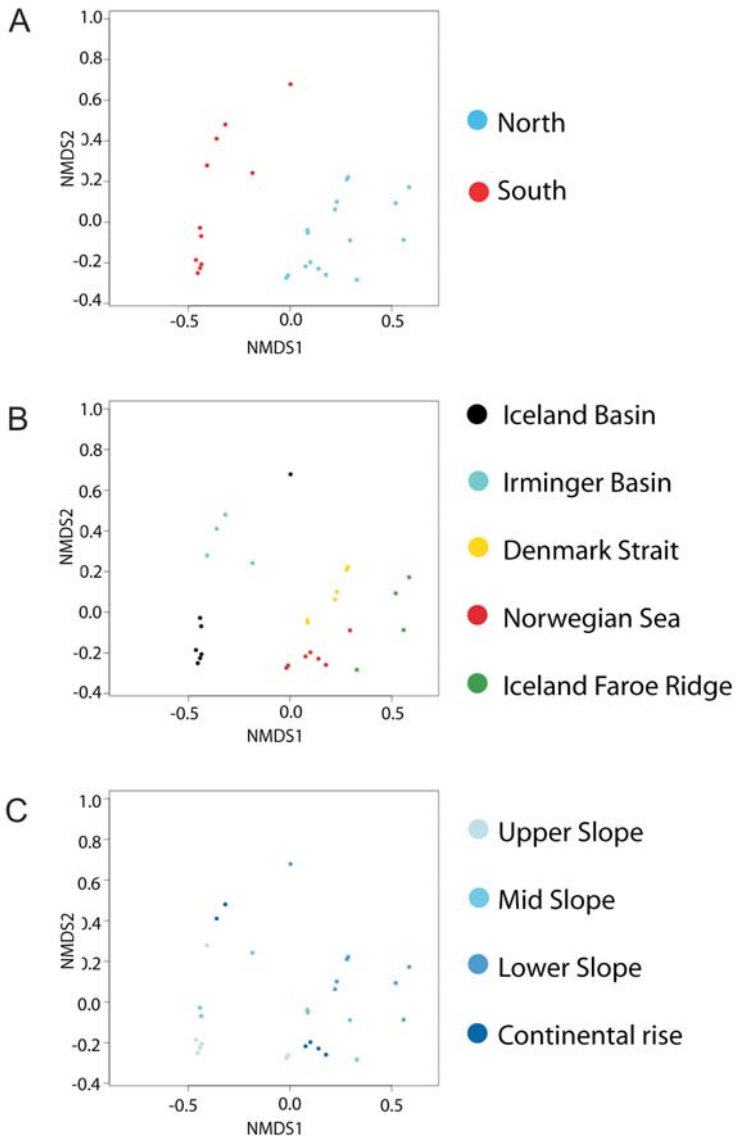

Fig. 3. NMDS displaying the variation of environmental conditions among sites. Bray-Curtis similarity performed on normalized data. Stress: 0.138993. **A**. North-South ($p = 0.001$, $R = 0.81544$). **B**. Regions ($p = 0.001$ and $R = 0.8253$). **C**. Depth gradients ($p = 0.001$, $R = 0.4981$).

sediments decrease from 0.06–0.12% and 0–0.39 µg/g, respectively, with increasing depth and distance from the coast (Table 2). Stations situated at the IFR and station #1215 are, in contrast to the Norwegian Sea, characterized by comparatively warmer bottom temperatures and higher bottom salinities (T: -0.6–1.33°C, S: 34.90–34.95) and are an indication for NSAIW as the main water mass (Table 1). The sediments are classified as sandy and sandy silt (Fig. 4). Here, sediments, which are represented

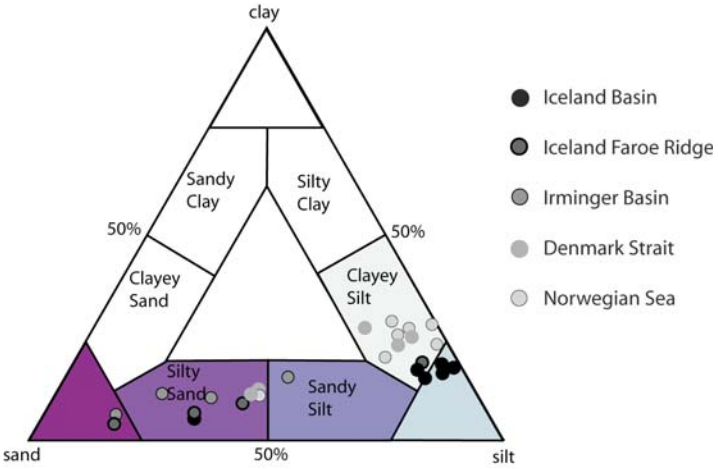

Fig. 4. Ternary plot of grain size distribution and classification (according to Shepard 1954), showing the regions where samples were taken (color of dots) and the grain size classification (color of cells).

by a maximum of 50% sand, have higher TOC (>1.2%), nitrogen (>0.15%), and chlorophyll *a* (> 0.17 µg/g, Table 2) concentrations, compared to sediments with more than 50% sand (chlorophyll *a*: 0–0.05%, nitrogen: 0.06–0.08%, TOC: 0.46–0.65%, Table 2). However, the station closest to the Icelandic coast is characterized by higher TOC, nitrogen and chlorophyll *a* contents (1.08%, 0.13% and 0.42%, respectively) and 50% sand in the sediments (Table 2).

The northernmost and deepest stations in the Denmark Strait (#1139, #1140) are characterized by bottom temperatures of -0.67°C and a bottom salinity of 34.91, which indicates NSDW as the dominant water mass (Table 1). This is where the silty sediments (Fig. 4, Table 2) contain the highest amount of TOC and nitrogen (TOC: ~0.83%, N: 0.09%) and intermediate chlorophyll *a* (0.04–0.05 µg/g). The shallowest stations in the Denmark Strait (#1127, #1128) show more than 50% silt with TOC and nitrogen above 0.5% and 0.05%, respectively. Here, chlorophyll *a* was the lowest (0.01 µg/g). The sediments between Greenland and Iceland closest to the Greenland Iceland Ridge (#1114, #1115, Table 2), have lowest nitrogen and TOC, but highest chlorophyll *a* values (Table 2). In comparison to the northernmost stations the stations between Greenland and Iceland show a comparatively higher bottom temperature. This area is mainly influenced by AW and PW, with slightly decreasing salinity towards the Greenlandic coast (Table 1).

The Irminger Basin is mainly influenced by two water masses. According to lower bottom salinity and temperature, the deep-sea sediments in the Irminger Basin are characterized by LSW (T: ~3°C, S: 34.94, Table 1), while the higher bottom temperature and salinity of stations closer to the GSR and Reykjanes Ridge indicate a mixture of LSW and MNAW. The sediments show a wide grain size distribution from sandy to silty sand (Fig. 4) and show a high amount of TOC (2.53–5.92%), but low nitrogen (0.02–0.05%). Chlorophyll *a* and the pigment

Table 2

Sediment data at the sampling sites. The multicore number refers to the stations illustrated in Table 1. The grain size distribution follows the Udden-Wentworth Scale (Wentworth 1922).

MUC number	Date	Longi-tude	Lat-itude	Sand [%]	Silt [%]	Clay [%]	TOC [%]	N [%]	C/N	Chloro-phyll *a* [µg/g]	Derivate pigments [µg/g]
959	28 Aug 2011	-21.5	60.05	6.17	78.08	15.75	0.67	0.09	7.44	0.02	0
971	29 Aug 2011	-19.89	60.18	10.62	74.89	14.48	2.14	0.08	26.75	0.03	0
974	30 Aug 2011	-18.14	60.34	10.67	75.14	14.18	0.8	0.06	13.33	0.01	0.02
987	31 Aug 2011	-18.7	60.93	3.09	79.92	16.99	3.46	0.11	31.45	0.03	0.01
1004	02 Sep 2011	-20.35	62.56	10.86	72.63	16.51	0.5	0.05	10.00	0.03	0
1014	03 Sep 2011	-20.79	62.93	5.14	77.03	17.83	0.62	0.09	6.89	0.05	0.06
1035	04 Sep 2011	-23.17	63.33	63.96	31.7	4.34	0.52	0.05	10.40	0.03	0.07
1050	05 Sep 2011	-31.37	61.62	57.49	33.01	9.5	5.92	0.03	197.33	0	0
1062	08 Sep 2011	-30.06	62.17	67.42	22.19	10.38	5.46	0.02	273.00	0	0
1065	08 Sep 2011	-28.08	63	79.5	15.14	5.36	2.53	0.02	126.50	0.01	0
1075	09 Sep 2011	-26.93	62.5	38.87	46.49	14.64	4.72	0.05	94.40	0.04	0.05
1114	13 Sep 2011	-26.27	67.21	46.85	41.83	11.33	0.43	0.04	10.75	0.06	0.08
1115	13 Sep 2011	-26.27	67.21	48.91	40.76	10.34	0.46	0.04	11.50	0.08	0.1
1127	14 Sep 2011	-26.75	67.65	16.85	56.1	27.04	0.64	0.07	9.14	0.01	0
1128	14 Sep 2011	-26.75	67.65	22.56	52.69	24.75	0.52	0.05	10.40	0.01	0
1139	15 Sep 2011	-23.7	67.84	8.07	67.32	24.61	0.83	0.09	9.22	0.04	0
1140	15 Sep 2011	-23.7	67.84	11.91	65.45	22.65	0.85	0.09	9.44	0.05	0.04
1151	17 Sep 2011	-9.93	69.09	10.28	61.28	28.45	5.26	0.06	87.67	0	0
1162	18 Sep 2011	-8.58	68.64	2.6	70	27.4	2.62	0.08	32.75	0.01	0.07
1164	18 Sep 2011	-6.96	67.59	3.9	73.44	22.66	2.85	0.09	31.67	0.01	0
1175	20 Sep 2011	-9.74	67.62	7.68	65.75	26.57	1.34	0.08	16.75	0.02	0
1177	20 Sep 2011	-12.17	67.65	16.25	64.14	19.61	1.29	0.08	16.13	0.39	0.43
1187	21 Sep 2011	-13.01	67.07	10.68	64.16	25.16	1.01	0.12	8.42	0.21	0.19
1215	22 Sep 2011	-12.37	66.3	47.53	42.4	10.06	1.26	0.16	7.88	0.17	0.19
879	31 Jul 2013	-8.57	63.1	63.38	30.94	5.68	0.65	0.08	8.13	0.05	0.07
880	31 Jul 2013	-8.15	63.39	81.34	15.93	2.74	0.46	0.06	7.67	0	0
881	01 Aug 2013	-7.71	63.58	9.43	72.48	18.09	1.23	0.15	8.20	0.36	0.35
882	02 Aug 2013	-10.97	63.42	51.8	39.99	8.2	1.08	0.13	8.31	0.42	0.44

derivates decrease with increasing depth from 0.04–0 µg/g and 0.05–0 µg/g, respectively. The C/N ratios vary among the study sites (Table 2). While in the Irminger Basin and one station in the Norwegian Sea the C/N ratio was high (Table 1, 94.4–273 and 87.67), the maximum ratio at the other stations was 32.75. Bottom oxygen was generally higher in the North compared to the South (Table 1).

Predictive models. — The models were generated based on 14 predictors and 28 sampled stations. The predictions extend over the whole Icelandic region (Figs 5–8).

RandomForest predictions are shown in Figs 5–8A, C, (E). Table 3 shows the prediction accuracy measures for the models. Mean squared residuals and percentage of variation explained are provided by the randomForest implementation in R of Liaw and Wiener (2002) (Table 3). As a more intuitive measure of prediction

Table 3

Prediction accuracy of random Forest models, showing randomForest mean squared residuals and explained variation, and Pearson's product moment correlation coefficient and adjusted R-squared of the linear relationship between predicted and observed data in the training dataset. All r and R-squared (RSq) values are significant at p <0.001

	Mean squared residuals	Variation explained (%)	Pearson's r	Adjusted RSq
Clay	21.12	64	0.9444	0.8879
Sand	364.23	44	0.9193	0.8392
Silt	216.76	44	0.9186	0.8379
Carbon (TOC)	2.056	25	0.8325	0.6813
Nitrogen (N)	0.001	-5	0.9055	0.8132
C/N	3337.61	15	0.9013	0.8053
Chlorophyll *a*	0.019	-37	0.8796	0.7650
Derivate pigments	0.021	-31	0.8469	0.7064

accuracy we calculated the Pearson product moment correlation coefficient r, which was significant at p <0.001 for all models. Correlation between observed and predicted variables is high, ranging from 0.83 to 0.94 and is best for grain size classes, nitrogen and C/N (Table 3). The percentage of explained variance is expressed as adjusted R-squared of a linear regression between observed and predicted values (Table 3).Adjusted RSquared values range from 68% (TOC) to 88% (sand). All regression models were significant at p <0.001.

Figs 9–11 display details of the resulting MARS models. On the left column, a model selection plot shows how the coefficient of determination R-squared increased with additional number of terms used (blue dashed line). On the same plot it is shown how the Generalized R-squared behaves with increasing number of terms (black line). Normally a unimodal distribution is expected and the number of terms corresponding to the mode is used for the final pruned model (dotted vertical line). The middle column plot shows the cumulative distribution of the absolute residual values (the absolute difference between observed and predicted values) contributes cumulatively to the total unexplained variation. So for instance, from the graph in Fig. 9A (middle column) we can infer that of the absolute residuals of the model predicting percentage of sand are 8 or less in 90% of the observations. This means that the absolute error in 90% or the cases is up to maximal 8%. The right column shows the distribution of residuals for each model. See also Milborrow (2014) for details on how to interpret these graphs.

MARS model predictions are shown in Figs 5–8B, D, (F). Table 4 summarizes which predictors were finally used in MARS models for each variable and displays R-square (RSq) and Generalized R-squared (GRSq) values. While RSq informs about the variation explained by the model using all predictors and up to 6-fold interaction between them, GRSq informs about the variation explained by the pruned model which was finally used for prediction. In case of percentage of sand, we see that MARS model could explain up to 97% of the variance using all terms, but it ex-

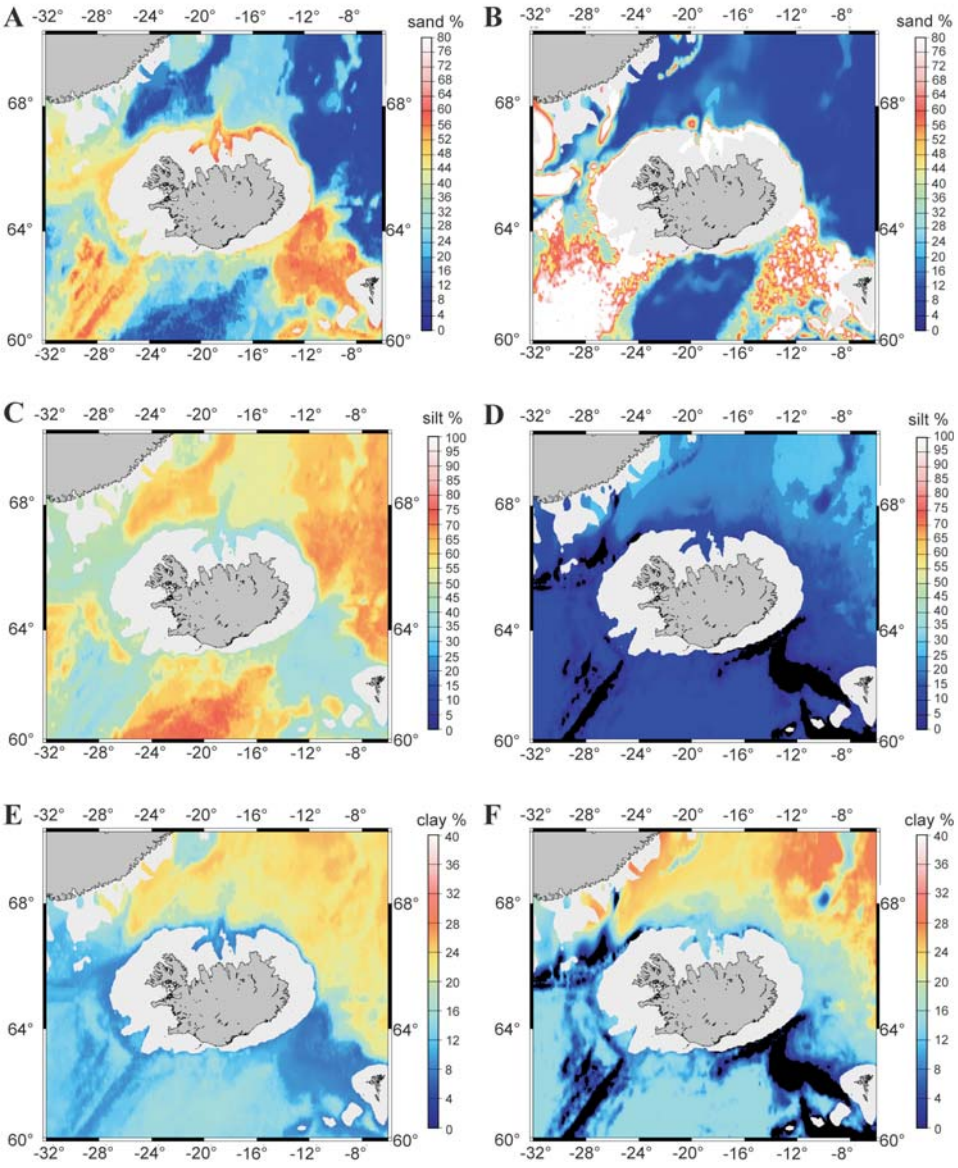

Fig. 5. RandomForest (A, C, E) and MARS (B, D, F) prediction of % sand (**A–B**); % silt **(C–D)**; % clay (**E–F**). The legend shows the scale used for the images.

plains only 83% of the variance with the final pruned model (see discussion). Relative grain size composition, total organic carbon and C/N ratio were predicted relatively well by MARS, having relatively high GRSq values (0.54–0.9). On the contrary nitrogen, chlorophyll *a* and pigment derivates display GRSq values lower than 0.25.

The modeling results show that coarse sediments are restricted to the areas near the Reykjanes Ridge, the Irminger Basin as well as the GIR and IFR (Fig. 5A–B),

Table 4

Independent (predictor) and dependent (response) variables used for MARS models (interactions between predictors not shown). R-squared (RSq) and Generalized R-squared (GRSq) are explaines in the results.

Response Predictor	Sand	Silt	Clay	TOC	N	C/N	Chlorophyll *a*	Derivate pigments
Temperature (interannual mean)					X			X
Temperature (interannual maximum)	X	X						X
Temperature (interannual range)	X	X	X		X	X		
Temperature (interannual minimum)							X	
Salinity (bottom water)								
Oxygen (bottom water)	X		X		X	X		
Sediment thickness	X	X		X		X		
POC (particulate organic carbon flux)				X		X		X
SVI (POC seasonal variation index)	X	X						
Currents (magnitude)								
Currents (maximum)			X	X				
Currents (mean)							X	X
Currents (minimum)					X		X	X
Depth				X		X		
GRSq	0.83	0.85	0.58	0.54	0.22	0.90	0.24	0.20
RSq	0.97	0.96	0.78	0.87	0.78	0.95	0.60	0.47

whereas the north is represented by finer sediments, comprising a high amount of clay and silt (Fig. 5C–F). The deep Norwegian Sea and the north-western Denmark Strait showed highest silt contents of the sediments (up to 60% in randomForest, ~30% in MARS models, Fig. 5C–D). Compared to the Faroe Bank Channel and the Irminger Basin, the deep Iceland Basin is characterized by fine sediments (Fig. 5A–C).

The percentage of sand, silt and clay were modeled independently from each other by both MARS and randomForest. Thus, the values of the three grain size classes should add up to 100 if the models predict accurately. Table 5 shows the summary statistics of the sum of predicted percentage of sand, silt and clay on the 22139 locations used for prediction for MARS and randomForest. Both modeling approaches display a median close to 100. Standard deviation is small in randomForest (1.47) but very high in MARS (1623.3). RandomForest displays a mean value of 100, but the mean value of MARS is highly biased (280.57) due to very high maximum values. Finally the residuals plotted in geographic space in Fig. 6A–B (note that the range -1 to +1 are white in these plots) show that virtually the whole area is over- (sum of three grain size classes above 100%) or underestimated (sum of the three grain size classes below 0%) in MARS model, but large geographic areas (white areas) in the randomForest model show a deviation of less than 1% from expected values. Remarkably the deep-sea areas North of Iceland are slightly overestimated in randomForest while they are underestimated in MARS. Typical range of variation is depicted in the histograms in Fig. 6C–D, being in the range of 96–105 in randomForest, but 60–140 in MARS.

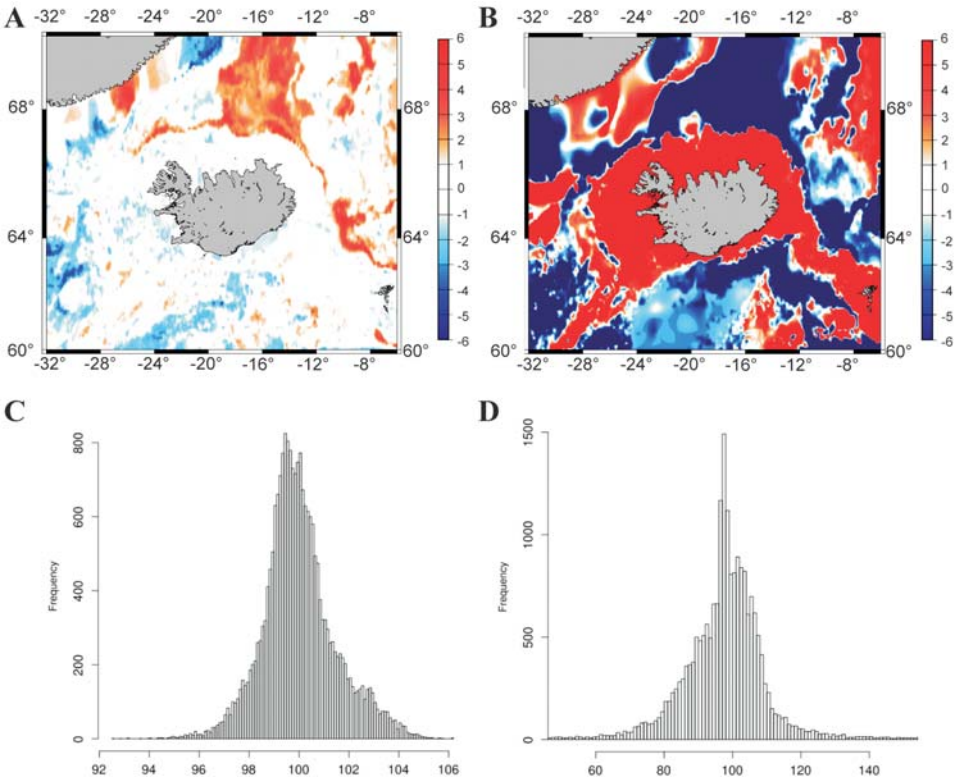

Fig. 6. Residuals of model performance (deviation from 100% of the sum of predicted % of sand, silt and clay) of randomForest (**A**) and MARS (**B**). Histogram of predicted sum of sand, silt and clay randomForest (**C**) and MARS (**D**).

The generated models for TOC, nitrogen and C/N ratio show differences between the studied areas (Fig. 7). The predicted TOC content varies between 0 and 6%, with even negative values predicted by the MARS model (black color in Fig. 7B). The lowest content is found along the GSR (~1.5% randomForest and ~1% in MARS models, Fig. 7A–B) and slightly higher values for TOC on the Reykjanes Ridge (Fig. 7A–B). The highest TOC content is predicted in the Iceland Basin, Irminger Basin and Norwegian Sea (TOC >1.5% in both models). The randomForest model predicts high values of nitrogen in the coastal areas, north of the GSR (N >0.08%), whereas the MARS model shows a prediction less than 0% at the shallow stations (black color in the figures). In both models the

Table 5

Comparison of randomForest and MARS models on sediment grain size prediction.

	Min	1st Qu	Median	Mean	SD	3rd Qu	Max
MARS	-79.41	92.06	98.42	280.57	1623.3	105.23	148448.53
randomForest	92.58	99.15	99.87	100	1.47	100.70	106.10

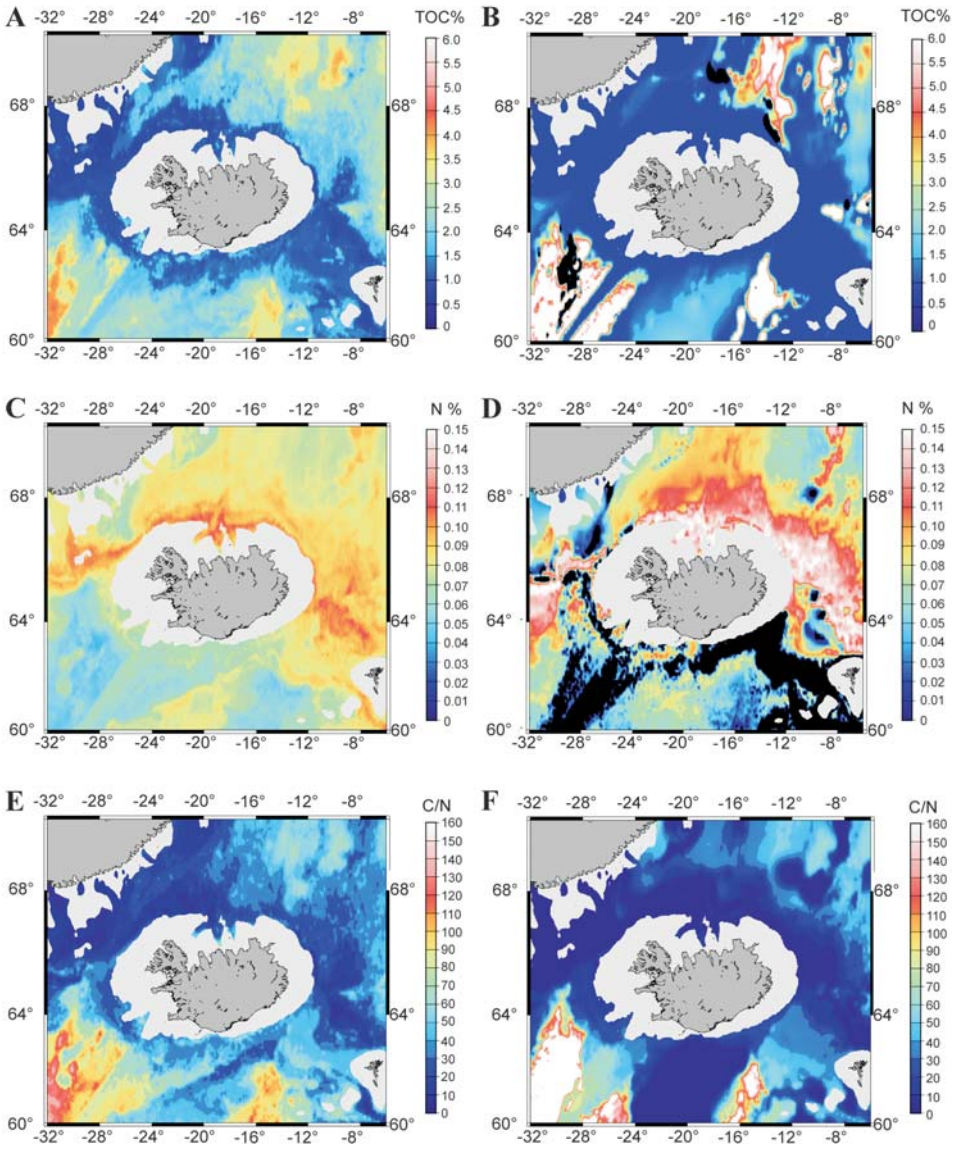

Fig. 7. Same as Fig. 5. % TOC in the sediments (**A**–**B**); % nitrogen in the sediments (**C**–**D**); calculated C/N ratio (**E**–**F**). The black parts in the MARS model for TOC and nitrogen refer to predicted negative values.

shelf areas (ridge and coast) differ from the deeper basins. RandomForest and MARS models predict higher C/N ratio in the Irminger Basin and the Iceland Basin (90–160 in random Forest and even higher in MARS (Fig. 7E–F). A smaller C/N ratio is predicted north of the GSR and the GSR (Fig. 7E–F).

The randomForest predictions on the pigments show that there is a high chlorophyll *a* and pigment derivative concentration present at the IFR, GIR, Reykja-

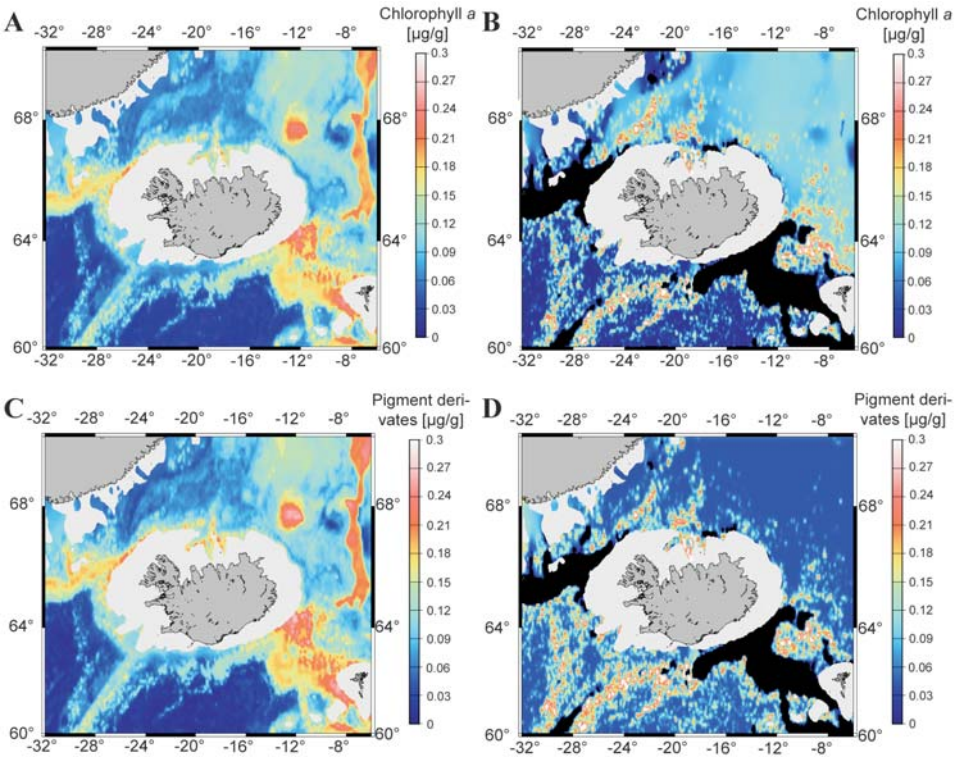

Fig. 8. Same as Fig. 5. Amount of chlorophyll *a* in the sediments in µg/g (**A**–**B**); amount of pigment derivates in the sediments in µg/g (**C**–**D**) . The black parts in the MARS model for TOC and nitrogen indicate predictions with negative values.

nes Ridge and in the eastern parts of the Norwegian Sea (0.12–0.3 µg/g, Fig. 8A). On the contrary, MARS predicts no pigments along the GSR and the Reykjanes Ridge (black color). Both models predict high chlorophyll *a* in the deep Norwegian Sea (Fig. 8A–B) but lower chlorophyll *a* in the southern Iceland Basin. In the randomForest model, chlorophyll *a* and pigment derivates appear to be almost similar (Fig. 8A, C), which differs in the MARS model approach. Here, the pigment derivates are predicted with a smaller variation west and east of the Reykjanes Ridge (0.07–0.3 µg/g *versus* 0.01–0.3 µg/g) and higher values in the South compared to the North (Fig. 8B, D).

Discussion

During the last decades, a number of studies have improved our knowledge of the deep-sea currents and water masses around Iceland (Hansen and Østerhus 2000; Pickart *et al.* 2005; Våge *et al.* 2011, 2013). Technologies like Acoustic Doppler Current Profilers (ADCPs) (Jochumsen *et al.* 2012; Våge *et al.* 2013) were used for

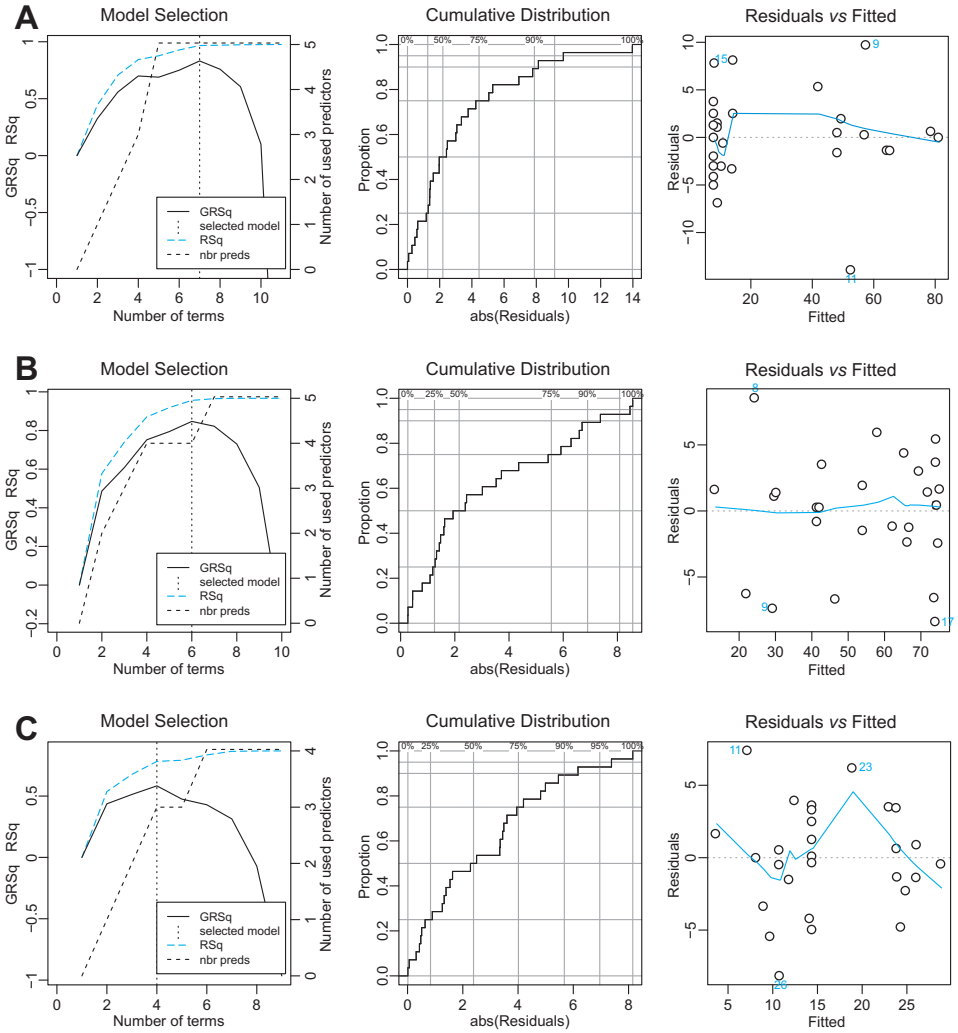

Fig. 9. MARS model performance plots. Left column: "model selection plot" showing distribution of RSq and GRSq with increasing number of terms, and selected model, middle column: cumulative distribution of prediction error; right column: residual plot showing outliers (labeled with numbers). Sand (**A**), silt (**B**), and clay (**C**).

detailed description of current velocities (for water mass formation and detailed descriptions of its transport see Swift 1980; Swift and Aagaard 1984; Swift *et al.* 1984; Hansen and Østerhus 2000; Pickard *et al*. 2005; Våge *et al*. 2011, 2013).

For the present study data were collected with CTD and MUC to analyze the conditions present at the time of sample collection and to predict the sediment grain sizes and organic matter in the study area for future studies on the deep-sea ecology, including species distribution, diversity and abundance. The amount of total organic carbon in the deep sea varies geographically, and is described by

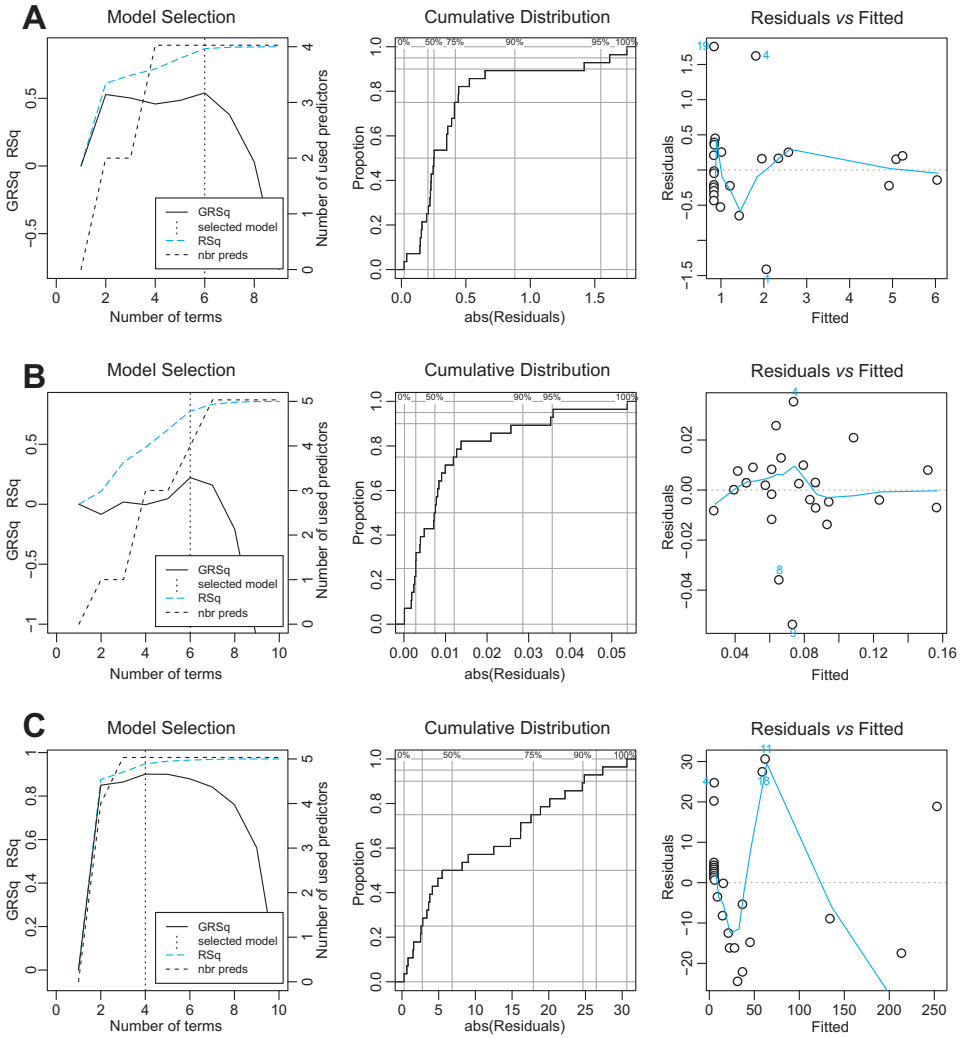

Fig. 10. MARS model performance plots. Left column: "model selection plot" showing distribution of RSq and GRSq with increasing number of terms, and selected model, middle column: cumulative distribution of prediction error; right column: residual plot showing outliers (labeled with numbers). TOC (**A**), nitrogen (**B**), C/N ratio (**C**).

Cranston (1997), Sauter *et al*. (2001) and Schubert and Calvert (2001) for the North Atlantic and the Arctic Ocean. Similar values are found in the present study (0.43–5.46%, Table 2).

The coarse sediments (more than 30% sand, Table 2) and high TOC (Table 2) in the Irminger Basin are a result of two strong bottom currents (~1 ms^{-1}), which transport the cold Arctic Water from the North across the ridge into the Atlantic Ocean (Jochumsen *et al*. 2005; Våge *et al*. 2011, 2013). The DSOW (Fig. 1) flows across the Denmark Strait into the Atlantic Ocean, where it rapidly sinks down to

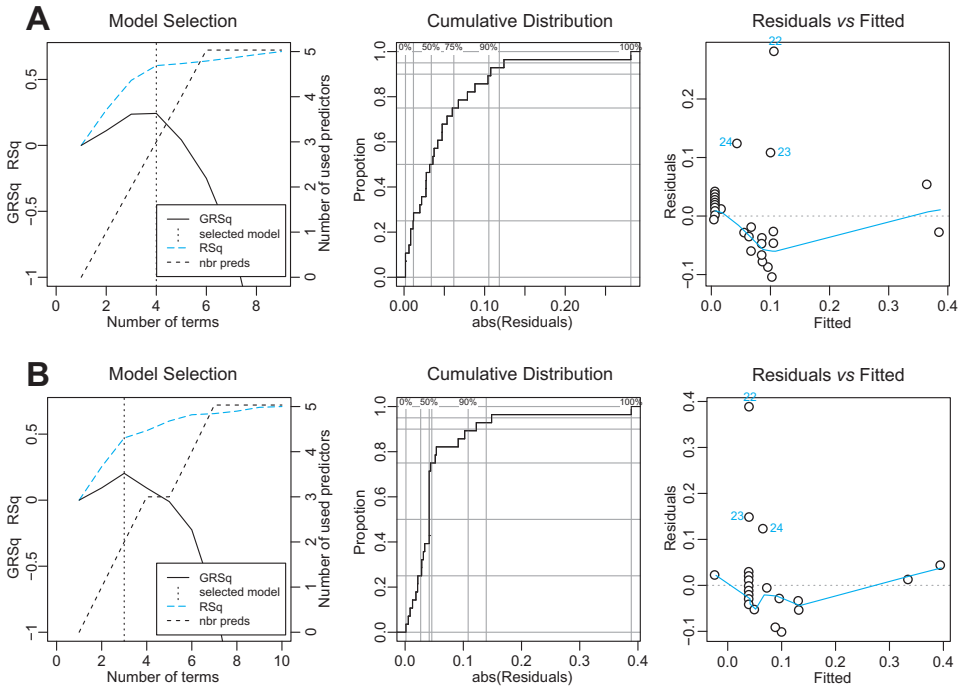

Fig. 11. MARS model performance plots. Left column: "model selection plot" showing distribution of RSq and GRSq with increasing number of terms, and selected model, middle column: cumulative distribution of prediction error; right column: residual plot showing outliers (labeled with numbers). Chlorophyll *a* (**A**), pigment derivates (**B**).

the bottom with a velocity of about 1 ms^{-1}. The DSOW and the ISOW (~1 ms^{-1}) from the east, which flows along the Icelandic coast and the Reykjanes Ridge and then north again into the Irminger Basin, explain the coarse sediments and the low nitrogen amount present in the Irminger Basin. Compared to that, the TOC is found to be high in that region, which can be explained by the high amount of foraminifera shells in the sediments (personal observation). The correlation of high numbers of foraminiferans (*Cibicides lobatulus* (Walker *et* Jacob, 1798)) with coarse sediments is also described from areas south of Kolbeinsey Ridge, where strong bottom currents occur (Lackschewitz and Wallrabe-Adams 1991). A study east of Greenland supports the present results. Johnson et al. (1975) found coarse sediments related to high turbidity currents between Cape Farewell and the Denmark Strait. However, Sommerhoff (1973) described silty and clayey sediments south of Greenland near the coast, where the effect of the outflow is lower. The Denmark Strait itself consists of silty sediments. The influence of the less strong EGC (0.25 ms^{-1}), a surface current that can reach down to about 200–300 m (Fischer, pers. comm.), can explain the coarser sediments and the less saline water at the station closest to the Greenland coast and are also described in a study near the Greenland coast in the northern Denmark Strait (Thies and Thiede 2004).

The deep Norwegian Sea is characterized by silty sediments with decreasing chlorophyll *a* and nitrogen but increasing TOC from the shallow coast to the deeper areas. Small grain sizes are also described in the northern Norwegian Sea (Pittenger *et al.* 1989; Kassens and Sarnthein 1989) and can be related to the absence of strong bottom currents in that area (Fig. 12). The decrease of TOC, nitrogen and chlorophyll *a* from the coast to the deep sea, which is observed in some regions, was already described in previous studies (Thistle *et al*. 1985; Wakeham *et al*. 1997; Gooday 2001; Rex *et al*. 2005, 2006; Smith *et al*. 2008) and explained by the uptake and degradation through the water column and the distance from the coast.

Towards the IFR the presence of the ISOW, which flows at ~1ms^{-1} across the IFR (Fig. 1), change the conditions in comparison to those found in the Norwegian Sea (ANOSIM, Fig. 3). Sediments along ridges are generally poorly sorted (Horowitz 1974; Ludwig *et al.* 1976; Lackschewitz and Wallrabe-Adams 1991; Talwani and Udintsev 2004). Down to 1000 m depth there is a lot of variation in the grain sizes, while stations below 1,000 meters feature a high amount of silt but less sand (Ludwig *et al*. 1976; Thies and Thiede 2004). Moreover, it was observed that sediments are influenced by hydrodynamic processes with finer sediments being more easily swept out (Lackschewitz and Wallrabe-Adams 1991). This supports the present results with silty sediments at the deepest stations and coarse sediments at the shallow stations (Fig. 12) and can be related to the ISOW, which flows across the IFR, sweeping out the smaller sediments from the ridge.

The hydrodynamic processes in the Iceland Basin were described by Bianchi and McCave (2000), who studied the Björn and Gardar Drifts south of Iceland. The fine sediments found at the drifts are related to the outflow of the ISOW from the IFR into the North Atlantic (see Bianchi and McCave 2000). There the ISOW follows the topography, before it flows south along the Reykjanes Ridge. Sediments, which are winnowed out by the ISOW are settling down in the deeper part of the Iceland Basin (*e.g.* as formation of Björn and Gardar Drifts), whereas the coast mainly comprises coarse sediments, due to the strong bottom current (Fig. 12).

In the present study, the related C/N ratios varied from 7 to 273 (Table 2). Sediments with a ratio between 7 and 8 derive from marine sediments (*e.g.* Müller 1977; Stein *et al.* 1994), whereas C/N ratio higher than 15, as found *e.g.* in the Irminger Basin, indicate an input of terrigenous material (*e.g.* Johnson *et al.* 1975; Hedges *et al.* 1986; Stein *et al.* 1994). Another study separated the higher C/N ratio into regions up to 1000 m (C/N = 10) and regions of 1500 m depth (C/N = 15) (Müller 1977) and support the present results in the deep Norwegian Sea and the Irminger Basin (Table 2). At the west coast of the US, Keil *et al.* (1994) described high C/N ratio in areas with coarse sediments, but a low C/N ratio in sediments with smaller grain sizes, which supports our results.

The hydrodynamic conditions explain the sediment distribution and the organic materials found in the sediments. Regional differences of the sediments among the

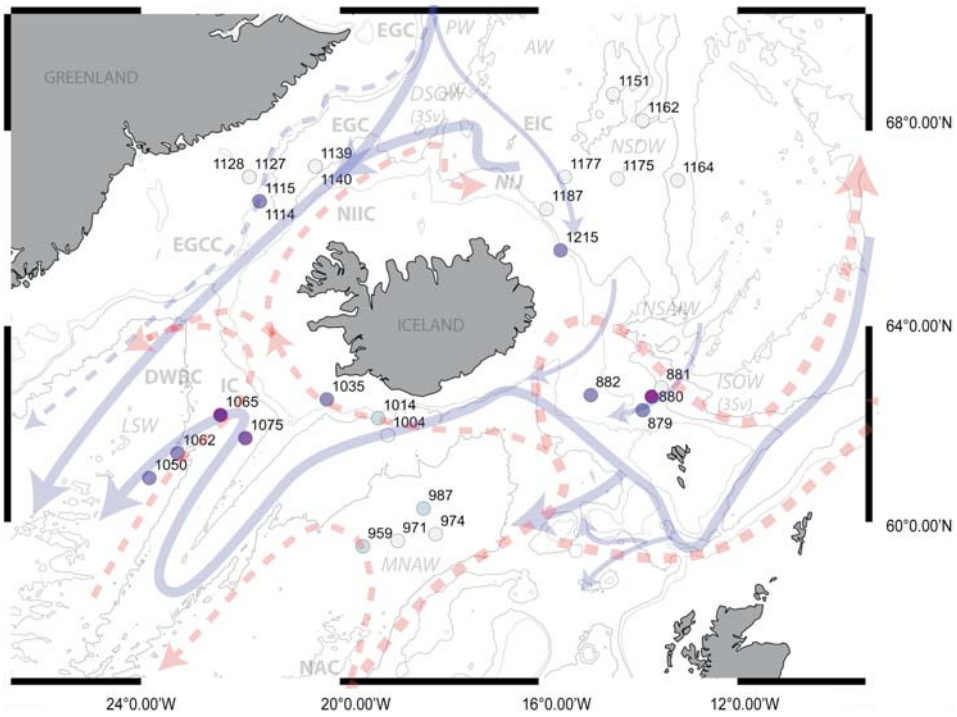

Fig. 12. Figs 1 and 2 combined to visualize the effect of the bottom currents on the sediment grain size distribution. Abbreviations are according to Fig. 1.

study sites are explained by the turbidite and contourite variability (Haskell and Johnson 1993; Brandes 2011), water depth and the distance from the coast (Thistle *et al*. 1985; Rex *et al*. 2005, 2006; Smith *et al*. 2008). Turbidites are fine sediments, derived from turbidity currents and are found in the Norwegian Sea. In contrast, contourite sediments, which are found south of the GSR in the shallow Iceland Basin and the Irminger Basin, show a high influence of bottom current activity.

The hydrodynamic conditions explain the sediment distribution and the organic materials present in the sediments. Studies focusing on the benthic community structure and abundance revealed that temperature, salinity and sediment grain sizes are among the most important factors in shaping communities (*e.g.* Rex *et al*. 2005; Brix and Svavarsson 2010). Hence, changes of the environmental conditions around Iceland will likely result in changes within the whole ecosystem.

RandomForest *versus* MARS models. — According to the percentage of variation explained by the model (Table 3), randomForest performed apparently bad in regression mode at first glance (but see below). The values are however comparable to other studies (*e.g.* Bachmair and Weiler 2012). The variation explained for grain size (sand, clay, silt) was best with 44–64% (Table 3). Organic carbon and C/N performed badly with 15–25%. Other variables display even negative values. Interpretation of the output of randomForest regression is, however,

still poorly understood. Furthermore, it is specifically misleading if terms are assumed to be equivalent to linear regression (Grömping 2009), but see Biau (2012) for an evaluation of its mathematical properties. While negative values in explained variance are not defined in linear regression, they can happen as negative explained variation in randomForest. In the randomForest implementation of Liaw and Wiener (2002) used here, it is computed on the (mean) Out Of Box error estimate (OOB) using the formula 1-MSE(OOB)/ var(y).

MSE(OOB) is a method for variation explanation computed as a mean sum of errors of the model prediction on the portion of the data that were randomly excluded to build the model (OOB) across all calculated random trees. Therefore, negative values of variation explanation occur when the mean error is larger than the variance of the response variable. Intuitively low or negative values should be interpreted as low performance of the predictors used. However, comparison of observed *versus* predicted values using Pearson's correlation coefficient and linear regression show a better picture. All randomForest models show significant high correlation between the predicted variables and the observed variables used for training (Table 3). Furthermore, adjusted RSq shows that the percentage of variance explained by the models is high (68–88%).

MARS models performed relatively well with the training dataset (Figs 5–8B, D, E). RSq values range from 0.47 (Derivate pigments) to 0.97 (sand), with values of sand, clay, and C/N above 0.9 (Table 4). However, very good coefficient of determination in the training datasets can produce over-fitted models that will perform badly on new datasets. In order to avoid this, MARS models were pruned by subsequent reduction of the number of terms. The final model is chosen by applying Generalized Cross Validation (GVC) on the pruned models (Figs 9–11). The error of the pruned models is expressed as standardized GVC and called GRSq (Figs 9–11, left column). This measure is analogous to RSq (R^2) and should be an indicator of how good the model will perform on new data (Milborrow 2014). The idea behind this is, that less complex models (models with less terms) should be more general and so perform better on new data than models that achieve a better fit to the training dataset by adding more terms. Interpretation of the model graphs can be consulted in Milborrow (2014). GRSq for our models ranged from 0.20 (Derivate pigments) to 0.90 (C/N). However, the models generally failed to extrapolate to areas outside the environmental envelope of the training dataset.

In general there is great congruence of randomForest and MARS models and results are meaningful in an oceanographic context. Model performance comparison between MARS and randomForest was additionally tested by building the sum of the percentage of sand, clay and silt on the prediction dataset (Fig. 6A–D). Each of these 3 models was calculated independently, but in a real world scenario these values should add up to 100%. It is evident in Table 5, that randomForest outperforms MARS in this test, displaying a mean value of 100 and a small standard deviation of 1.47, *versus* mean = 280.57, SD = 1623.3 in MARS. Median values are

however similarly good in both approaches, but MARS showed much greater under and overestimation of values (see Min, Max).

In the areas outside the environmental envelope of the training dataset, regression splines tend to greatly over- and underestimate the values. RandomForest however seems to be more robust against it probably because of the non-linear nature of the models and the bagging step in producing the models. This is evidenced in the current exercise with variables representing a percentage value like sand, silt, and clay, which of course cannot be negative or over 100% at any site. MARS predicted for instance that the sum of these three variables values ranged between -79% and 148448% (Table 5), while randomForest predictions ranged from 92.58% to 106.10%.

Conclusion

Our study shows that 28 datapoints were able to produce acceptable predictions on a larger spatial scale.

While all layers presented here will be available at the online repository PANGAEA, we recommend to use the randomForest layers as predictors in further studies only. A corrected set of randomForest prediction layers in which sand, silt and clay values add up to 1 were made additionally available (PANGAEA: http://doi.org/10.1594/PANGAEA.833704). Although predictions show meaningful results, the models presented herein were calculated using a relatively small training dataset. We recommend the use of these layers as relative values at regional geographic scales only. However, the modeling output could be improved by more sampling in the shallow areas, along further ridge systems (*e.g.* Reykjanes Ridge, Kolbeinsey Ridge) as well as in abyssal areas north and south of the GSR.

Acknowledgements. — First, we would like to thank the captains and their entire crews from the R/V *Meteor* and R/V *Poseidon*, without whom the sample collection would not have been possible at all. Thanks to all those who helped to take the samples aboard, especially the MUC team and Falk Huettmann (CTD data collection and introducing us to modeling approaches). For our laboratory work and the results gained for this study, we would like to thank Heike Rickels from the ICBM Terramare for the C/N analyses, Prof. Dr Gerd Liebezeit (ICBM Terramare, Wilhelmshaven) for the possibility to use the HPLC for pigment analyses and Jürgen Titschack from MARUM, Bremen for the ability to do the grain size analyses and for the nice discussions. The NISE data were kindly provided by the Marine Research Institute (Iceland), the Institute of Marine Research (Norway), the Faroese Fisheries Laboratory, the Arctic and Antarctic Research Institute (Russia), and the Geophysical Institute, University of Bergen (Norway). We also want to thank Dr Saskia Brix for giving the possibility to work in the frame of the IceAGE project. We really appreciated the help of Dr Jürgen Fischer from GLOMAR in Kiel, who helped to understand the complex physical oceanography in the study area. We thank the three reviewers for their great suggestions and corrections, which improved the final version of our paper.

References

BACHMAIR S. and WEILER M. 2012. Hillslope characteristics as controls of subsurface flow variability. *Hydrology and Earth System Sciences* 16: 3699–3715.

BIANCHI G.G. and MCCAVE I.M. 2000. Hydrography and sedimentation under the deep western boundary current on Björn and Gardar Drifts, Iceland Basin. *Marine Geology* 165: 137–169.

BIAU G. 2012. Analysis of a Random Forests Model. *Journal of Machine Learning Research* 13: 1063–1095.

BRANDES H.G. 2011. Geotechnical characteristics of deep-sea sediments from the North Atlantic and North Pacific oceans. *Ocean Engineering* 38: 835–848.

BREIMAN L. 2001. Random Forests. *Machine Learning*: 45: 5–32.

BRIX S. and SVAVARSSON J. 2010. Distribution and diversity of desmosomatid and nannoniscid isopods (Crustacea) on the Greenland–Iceland–Faeroe Ridge. *Polar Biology* 33: 515–530.

BROWN L.M., HARGRAVE B.T. and MACKINNON M.D. 1981. Analysis of Chlorophyll *a* in Sediments by High-Pressure Liquid Chromatography. *Canadian Journal of Fisheries and Aquatic Sciences* 38: 205–214.

CRANSTON R.E. 1997. Organic carbon burial rates across the Arctic Ocean from the 1994 Arctic Ocean Section expedition. *Deep-Sea Research II* 44: 1705–1723.

CUTTER G.A. and RADFORD-KNOERY J. 2013. Determination of Carbon, Nitrogen, Sulfur, and Inorganic Sulfur Species in Marine Particles. *In*: D.C. Hurd and D.W. Spencer (eds) *Marine Particles: Analysis and Characterization*. American Geophysical Union, Washington D.C. 63: 57–63.

DANOVARO R., DELL'ANNO A., FABIANO M., PUSCEDDU A. and TSELEPIDES A. 2001. Deep-sea ecosystem response to climate changes: the eastern Mediterranean case study. *Trends in Ecology and Evolution* 16: 505–510.

DIVINS D.L. 2003. *Total sediment thickness of the World's Oceans and marginal seas. Ver 1*. World Data Service for Geophysics, www.ngdc.noaa.gov/mgg/sedthick/sedthick.html

FRIEDMAN J.H. 1991. Multivariate Adaptation Regression Splines. *The Annals of Statistics* 19: 1–141.

GOODAY A.J. 2001. Biological responses to seasonally varying fluxes of organic matter to the Ocean floor: A review. *Journal of Oceanography* 58: 305–332.

GRÖMPING U. 2009. Variable Importance Assessment in Regression: Linear Regression *versus* Random Forest. *The American Statistician* 63: 308–319.

HANSEN B. and ØSTERHUS S. 2000. North Atlantic-Nordic Seas exchanges. *Progress in Oceanology* 45: 109–208.

HASKELL B.J. and JOHNSON T.C. 1993. Surface sediment response to deepwater circulation on the Blake Outer Ridge, western North Atlantic: paleoceanographic implications. *Sedimentary Geology* 82: 133–144.

HEDGES J.I., CLARK W.A., QUAY P.D., RICHEY J.E., DEVOL A.H. and DE M. SANTOS U. 1986. Compositions and fluxes of particulate organic material in the Amazon River. *Limnology and Oceanography* 31: 717 –738.

HOROWITZ A. 1974. The Geochemistry of sediments from the northern Reykjanes Ridge and the Iceland-Faroes Ridge. *Marine Geology* 17: 103–122.

JOCHUMSEN K., QUADFASEL D., VALDIMARSSON H. and JÓNSSON S. 2012. Variability of the Denmark Strait overflow: Moored time series from 1996–2011. *Journal of Geophysical Research*: *Oceans (1978–2012)* 117: C12003.

JOHNSON G.L., SOMMERHOFF G. and EGLOFF J. 1975. Structure and morphology of the west Reykjanes basin and the southeast Greenland continental margin. *Marine Geology* 18: 175–196.

KASSENS H. and SARNTHEIN M. 1989. Carbon, wet bulk density and grain size distribution of sediment core GIK23055-2 in the Norwegian Sea (Table 2). doi:10.1594/PANGAEA.418247. *In*: H. Kassens and M. Sarnthein, A link between paleoceanography, early diagenetic cementation, and shear strength maxima in Late Quaternary deep-sea sediments? *Paleoceanography* 4: 253–269.

KEIL R.G., TSAMAKIS E., BOR FUH C., GIDDINGS J.C. and HEDGES J.I. 1994. Mineralogical and textural controls on the organic composition of coastal marine sediments: Hydrodynamic separation using SPLITT-fractionation. *Geochimica et Cosmochimica Acta* 58: 879–893.

LACKSCHEWITZ K.S. and WALLRABE-ADAMS H.-J. 1991. Composition and origin of sediments on the mid-oceanic Kolbeinsey Ridge, north of Iceland. *Marine Geology* 101: 71–82.

LIAW A. and WIENER M. 2002. Classification and Regression by randomForest. *R News* 2: 18–22.

LOGEMANN K., ÓLAFSSON J., SNORRASON Á., VALDIMARSSON H. and MARTEINSDÓTTIR G. 2013. The circulation of Icelandic waters – a modelling study. *Ocean Science* 9: 931–955.

LUDWIG G., MÜLLER H. and VOLLBRECHT K. 1976. Sediments on the Iceland-Faeroe ridge. *Geologisches Jahrbuch* 16: 3–28.

LUTZ M.J., CALDEIRA K., DUNBAR R.B. and BEHRENFELD M.J. 2007. Seasonal rhythms of net primary production and particulate organic carbon flux to depth describe the efficiency of biological pump in the global ocean. *Journal of Geophysical Research* 112: 1–26.

MALMBERG S.A. and VALDIMARSSON H. 2003. Hydrographic conditions in Icelandic waters, 1990 – 1999. *ICES Marine Science Symposia* 219: 50–60.

MEIßNER K., FIORENTINO D., SCHNURR S., MARTINEZ ARBIZU P., HUETTMANN F., HOLST S., BRIX S. and SVAVARSSON J. 2014. Distribution of benthic marine invertebrates at northern latitudes – An evaluation applying multi-algorithm species distribution models. *Journal of Sea Research* 85: 24–254.

MILBORROW S. 2014 *Notes on the earth package. R package version 3.2-6*. http://CRAN.R-project.org/package:earth

MÜLLER P.J. 1977. CN ratios in Pacific deep-sea sediments: Effect of inorganic ammonium and organic nitrogen compounds sorbed by clays. *Geochimica et Cosmochimica Acta* 41(6): 765–776.

NIEUWENHUIZE J., MAAS Y.E.M. and MIDDELBURG J.J. 1994. Rapid analysis of organic carbon and nitrogen in particulate materials. *Marine Chemistry* 45: 217–224.

NILSEN J., HÁTÚN H., MORK K. and VALDIMARSSON H. 2008. *The NISE Dataset*. Technical Report 08-07. Tórshavn, Faroe Islands: 1–17.

OKSANEN J., BLANCHET F.G., KINDT R., LEGENDRE P., MINCHIN P.R., O'HARA R.B., SIMPSON G.L., SOLYMOS P., STEVENS M.H.H. and WAGNER H. 2013. vegan: Community Ecology Package. R package version 2.0-9. http://CRAN.R-project.org/package:vegan

PICKART R.S., TORRES D.J. and FRATANTONI P.S. 2005. The East Greenland Spill Jet. *Journal of Physical Oceanography* 35: 1037–1053.

PITTENGER A., TAYLOR E. and BRYANT W. 1989. Physical and geotechnical properties of Norwegian Sea sediments. doi:10.1594/PANGAEA.742919. *In*: A. Pittenger, E. Taylor and W. Bryant. The influence of biogenic silica on the geotechnical stratigraphy of the Vøring Plateau, Norwegian Sea. *In*: O. Eldholm, J. Thiede and E. Taylor (eds) *Proceedings of the Ocean Drilling Program, Scientific Results, College Station, TX (Ocean Drilling Program)* 104: 923–940.

REX M.A., MCCLAIN C.R., JOHNSON N.A., ETTER R.J., ALLEN J.A., BOUCHET P. and WARÉN A. 2005. A Source-Sink Hypothesis for Abyssal Biodiversity. *The American Naturalist* 165: 163–178.

REX M.A., ETTER R.J., MORRIS J.S., CROUSE J., MCCLAIN C.R., JOHNSON N.A., STUART C.T., DEMING J.W., THIES R. and AVERY R. 2006. Global bathymetric patterns of standing stock and body size in the deep-sea benthos. *Marine Ecology Progress Series* 317: 1–8.

SAUTER E.J., SCHLÜTER M. and SUESS E. 2001. Organic carbon flux and remineralization in surface sediments from the northern North Atlantic derived from pore-water oxygen microprofiles. *Deep-Sea Research I* 48: 529–553.

SCHNURR S., BRAND A., BRIX S., FIORENTINO D., MALYUTINA M. and SVAVARSSON J. 2014. Composition and distribution of selected munnopsid genera (Crustacea, Isopoda, Asellota) in Icelandic waters. *Deep-Sea Research I* 84:142–155.

SCHUBERT C.J. and CALVERT S.E. 2001. Nitrogen and carbon isotopic composition of marine and terrestrial organic matter in Arctic Ocean sediments: implications for nutrient utilization and organic matter composition. *Deep-Sea Research I* 48: 789–810.

SEITER K., HENSEN C. and ZABEL M. 2005. Benthic carbon mineralization on a global scale. *Global Biogeochemical Cycles* 19: 1–26.

SHEPARD F.P. 1954. Nomenclature Based on Sand-silt-clay Ratios. *Journal of Sedimentary Petrology* 24: 151–158.

SMITH C.R., DE LEO F.C. BERNARDINO A.F., SWEETMAN A.K. and MARTINEZ ARBIZU P. 2008. Abyssal food limitation, ecosystem structure and climate change. *Trends in Ecology and Evolution* 23: 518–528.

SOMMERHOFF G. 1973. Grain size distribution in sediments samples of station US_EXP_15, continental shelf and slope of southeast Greenland (Table 10). doi: 10.1594/PANGAEA.604850. *In*: G. Sommerhoff, Formenschatz und morphologische Gliederung des südostgrönländischen Schelfgebietes und Kontinentalabhanges. *Meteor Forschungsergebnisse, Deutsche Forschungsgemeinschaft, Reihe C Geologie und Geophysik, Gebrüder Bornträger. Berlin, Stuttgart* C15: 1–54.

STEFÁNSSON U. 1962. North Icelandic waters. *Rit Fiskideildar* 3: 1–269.

STEIN R., GROBE H., WAHSNER M. 1994. Organic carbon, carbonate, and clay mineral distributions in eastern central Arctic Ocean surface sediments. *Marine Geology* 119: 269–285.

SVAVARSSON J., STRÖMBERG J.O. and BRATTEGARD T. 1993. The deep-sea asellote (Isopoda, Crustacea) fauna of the Northern Seas: species composition, distributional patterns and origin. *Journal of Biogeography* 20: 537–555.

SWIFT J.H. 1980. The circulation of the Denmark Strait and Iceland-Scotland overflow waters in the North Atlantic. *Deep-Sea Research* 31: 1339–1355.

SWIFT J.H. and AAGAARD K. 1981. Seasonal transitions and water mass formation in the Iceland and Greenland seas. *Deep-Sea Research* 28A: 1107–1129.

SWIFT J.H., AAGAARD K. and MALMBERG S.-A. 1984. The contribution of the Denmark Strait overflow to the deep North Atlantic. *Deep-Sea Research* 27A: 29–42.

TALWANI M. and UDINTSEV G.B. 2004. *Grain size analysis of Hole 38-350*. doi:10.1594/PANGAEA.222164

THIES A. and THIEDE J. 2004. *Grain size distribution in surface sediments of the Norwegian Sea* (Table 2). doi:10.1594/PANGAEA.141304

THIES A. 1991. Die Benthos-Foraminiferen im Europäischen Nordmeer. *Berichte aus dem Sonderforschungsbereich 313* 31: 97 pp. Christian-Albrechts-Universität, Kiel.

THISTLE D., YINGST J.Y. and FAUCHALD K. 1985. A deep-sea benthic community exposed to strong near-bottom currents on the Scotian Rise (western Atlantic). *Marine Geology* 66: 91–112.

VÅGE K., PICKART R.S. SPALL M.A., VALDIMARSSON H., JÓNSSON S., TORRES D.J., ØSTERHUS S. and ELDEVIK T. 2011. Significant role of the North Icelandic Jet in the formation of Denmark Strait overflow water. *Nature Geosciences* 4: 723–727.

VÅGE K., PICKART R.S., SPALL M.A., MOORE G.W.K., VALDIMARSSON H., TORRES D.J., EROFEEVA S.Y. and NILSEN J.E.Ø. 2013. Revised circulation scheme north of the Denmark Strait. *Deep-Sea Research I* 79: 20–39.

VENABLES W.N. and RIPLEY B.D. 2002. *Modern Applied Statistics with S. Fourth Edition*. Springer, New York: 497 pp.

WAKEHAM S.G., LEE C., HEDGES J.I., HERNES P.J. and PETERSON M.L. 1997. Molecular indicators of diagenetic status in marine organic matter. *Geochimica et Cosmochimica Acta* 61: 5363–5369.

WEISSHAPPEL J.B. and SVAVARSSON J. 1998. Benthic amphipods (Crustacea: Malacostraca) in Icelandic waters: diversity in relation to faunal patterns from shallow to intermediate deep Arctic and North Atlantic Oceans. *Marine Biology* 131: 133–143.

WENTWORTH C.K. 1922. A scale of grade and class terms for clastic sediments. *Journal of Geology* 30: 377–392.

Received 7 March 2014
Accepted 15 June 2014